Plasma Chem Plasma Process
DOI 10.1007/s11090-017-9802-1

REVIEW ARTICLE

Atmospheric Plasma Spraying Evolution Since the Sixties Through Modeling, Measurements and Sensors

P. Fauchais[1] · M. Vardelle[1] · S. Goutier[1]

Received: 28 October 2016 / Accepted: 16 February 2017

Abstract This paper presents, through examples, the evolutions of atmospheric plasma spraying since the sixties. The drastic improvement of the spray conditions and coatings reproducibility during more than 50 years was linked both to researches in laboratories and developments of spray equipment's (plasma torches, computerized control panels, robots to spray coatings on complex parts, sensors working in the harsh environment of spray booths…). This evolution is illustrated through the following topics: (1) plasma forming gas thermodynamic and transport properties either at local thermodynamic equilibrium or more recently at two temperatures; (2) evolution of plasma spray torches since the nineties; (3) plasma jet and in-flight particle measurements with laboratory equipment's and then sensors in spray booths; (4) plasma jets and torches modeling as well as heat and momentum transfer to particles; (5) splats formation and layering.

Keywords Plasma spraying · History · Spray conditions improvement

Introduction

According to Tucker [1] the industrial applications of atmospheric plasma spraying particles in the tens of micrometer size range using direct current (DC) plasma torches, appeared at the beginning of the fifties, about one year after the D-Gun (detonation) process. In the sixties the inductively coupled Radio Frequency plasma torches showed up but were developed [2] in the seventies. As they are mainly used for powders spheroïdization, we will not consider them. DC plasma spraying under controlled atmosphere was developed on an Industrial scale in 1974 by Muehlberger [3] for low pressure

✉ M. Vardelle
michel.vardelle@unilim.fr

[1] European Ceramics Center, University of Limoges, CNRS, SPCTS UMR 7315, 87000 Limoges, France

Published online: 23 February 2017

plasma spraying. Later in the nineties, installations for spraying non-oxide ceramics in argon atmosphere at atmospheric pressure were developed, by the CEA (Commissariat à l'Energie Atomique) and then by Plasma Technik [4, 5].

In the following we will only consider plasma spraying at atmospheric pressure, either in air or controlled atmosphere. The industrial use of these atmospheric DC torches really started to grow in the sixties and the first applications were in aircraft engines and nuclear reactors.

Plasma sprayed coating qualities depend on [2]:

- Plasma jet formation linked to the torch design, the plasma forming gas composition and mass flow rate, the dissipated power, and few other process parameters. Very important features are arc root fluctuations at the anode and also the electrodes erosion velocity;
- Powder characteristics such as the sprayed powder chemical composition, particle size distribution and morphology (depending on the powder manufacturing process);
- Powder injection system, including the injector position, internal diameter, shape, length and tilting as well as on the connecting hose length and "trajectory" between the powder feeder and injector;
- Substrate material and preparation, including cleanliness and roughness, oxidation state oxide composition and thickness…), preheating time and temperature, as well as temperature control during and after spraying;
- Relative motion of the torch-substrate, which controls the coating thickness per pass and, partially, the heat transferred to coating and substrate

Up to the eighties, the development of plasma spraying was carried out in an empirical manner. It mainly consisted in (1) varying the operating spray parameters, for a powder with particles of given morphology and size distribution and, (2) characterizing the properties of the resulting coating and evaluating its performance under specific use conditions. This method was repeated until certain standards were obtained and the spray parameters was settled [2, 6, 7]. The quality of coating, the microstructure and service properties are important because it permits high reproducibility, narrow variability, predictable performance and lifetime thus reducing rework, warrantee costs and liability risk, which of course promote customer satisfaction.

In parallel to these empirical developments, modeling and measurements of plasma jets (temperatures and velocities) and in-flight particles (trajectories, temperatures and velocities) were developed in laboratories. Obtained results have progressively transformed the conventional plasma spray process from an art to a science. These measurements at the end of nineties and at the beginning of the new millennium have permitted to follow the impact, flattening and solidification of one particle (splat formation) and through splats layering, a better control of coating morphologies and thus thermo-mechanical properties achieved.

All these laboratory works have demonstrated the importance of the better control in real time of temperatures and velocities of both the plasma jet and in-flight particles. For example the torch voltage decrease with the electrode erosion, especially that of anode, plays an important role on coating properties evolution. However, measurements of in-flight particles demonstrated that best results were obtained by increasing the arc current and not by modifying flow rates of plasma forming gases. However it is only at the beginning of the nineties that appeared in spray booths computerized systems, controlling the macroscopic spray parameters (flow rates of plasma forming gases, arc current and

voltage). It made possible to follow continuously the spray process at the macroscopic level and for example to keep the plasma enthalpy constant in spite of electrode erosion.

In the nineties also, according to the improvement of coating qualities obtained in laboratories with sophisticated measurements of plasma jets and particles in-flight, sensors were developed to achieve similar controls in the harsh environment of spray booths. Of course the better knowledge of the key parameters controlling plasma sprayed coatings has in parallel promoted the development of plasma torches adapted to higher deposition rates, with much less arc root fluctuations and higher power levels.

In parallel to laboratory research development of plasma torches and process controls have been lead by entrepreneurial individual companies [8]. Vacuum plasma deposition, under-water spraying, RF plasma spraying, high power blown arcs, high velocity plasmas (for example PlazJet), multi-cathode torches, central powder feed guns, reactive plasma spray forming for example were developed. The papers of Dzulko et al. [9] and Marquès et al. [10] give an excellent review of the different plasma torches developed.

The erosion of electrodes and the way to control it through working parameters was also intensively studied [11, 12].

In the new millennium also the development of new spray techniques, suspensions or solutions, producing coatings with nanometer structures became one of the favorite laboratory aims [13, 14].

The development of models and measurements has required calculations of thermodynamic, transport and radiation properties of the different plasma forming gases first at equilibrium and later, in the nineties, at two temperatures.

This paper presents the evolution of measurements and modeling of the plasma spray process during almost 60 years, with:

- A short story of the evolution of calculations of plasma properties,
- Plasma spray torches,
- Plasma jet measurements,
- In-flight particles measurements,
- Plasma jets and plasma torches modeling
- Modeling heat and momentum transfer to particles
- Splats formation and layering.

Plasma Properties

According to the numerous papers published about thermodynamic and transport properties only a few examples will be presented.

Local Thermodynamic Equilibrium

The composition of plasma at given temperature, T, and pressure, p, can be found from the solution of the Gibbs–Duhem relationship [15–19]. The Gibbs free energies and/or the chemical potentials are calculated either by using standard thermodynamic tables [16–19] or through partition functions. However the partition function values and their derivatives are very sensitive to the limitation theories used for their calculation [20]. However, when using the same limitation theory for all components of plasma, its composition and thermodynamic properties are not very different (less than 4% for the major species) from

those calculated using another limitation theory [20–22]. This is due to the fact that when limitation theories play an important role (for example, at $T > 13000$ K for an argon atom), the density of the considered species is already low. But using different limitation theories for the different plasma components could introduce rather significant errors (up to 30%) in the composition and thermodynamic properties. It is therefore important for properties at $T > 8000$ K to use data from only one source, if possible.

The compositions of gases most commonly used in plasma torches such as: argon, nitrogen, hydrogen, helium, oxygen, air, water… have been calculated see for example [20–27]. Calculations were also performed for gases containing metal vapor due to electrode erosion, see for example [28]. Of course, specific heat at constant pressure, enthalpy, and sound velocity were also calculated see for example [29].

Calculation of the transport coefficients is by far more complex because it implies taking into account the velocity distributions, the fluxes (mass, momentum, and energy) of all species through a reference surface *dA* moving with the mean fluid velocity. The theory of the transport properties of gas mixtures is based on solving the Boltzmann integral differential equations by the Chapman–Enskog method [30] applied to complex mixtures. Hirschfelder et al. [31] has developed this calculation for weak ionized gases, and different authors demonstrated they were valid for thermal plasmas [32, 33]. However the collision integrals are not always well known, as well as partition function calculation and large uncertainties may result [33]. Such data are very important for plasma processes modeling [34]. For plasma spray forming gases have been published for example:

- Electrical conductivity, σ, of Ar, H_2, Ar–H_2, Ar–He, Ar–N_2, N2, O_2, H_2O, air [24, 26, 35–39]… and also Ar–Fe, air–Cu [26, 28, 40]… (metal vapors modifying drastically σ [41]),
- Viscosity, μ, of air, Ar–H_2, N_2–H_2, Ar–He [24, 26, 38, 39], Ar–Cu, air–Cu [37, 40]…
- Thermal conductivity of air, Ar–H_2, Ar–He, N_2–H_2, H_2O [26, 35, 38, 41]…
- Diffusion coefficients for Ar–H_2 [39], Fe in air [42], Cu in air [43]…
- Radiation mechanisms in plasmas [26, 44–46]: lines and their width, volumetric spectral emission, continuum radiation for plasma gases without [26, 44–46] or with metal vapors [47, 48]… effective or net emission coefficient (NEC) of the plasma, which is a means of taking into account self-absorption in plasmas with total volumetric emission coefficients of gases such as argon, nitrogen, hydrogen, helium, air, water vapor, and their mixtures at atmospheric pressure over the temperature range from 5000 to 25,000 K [47–51]…

Thanks to all these data, many of them being obtained in the nineties and at the beginning of the millennium, the plasma flows and the corresponding heat and momentum transfers to particles were modeled and results compared to measurements.

Non-equilibrium Calculations

In the course of the development of thermal plasma technology, the assumption of local thermodynamic equilibrium (LTE) in the hot regions of the plasma has been generally accepted, even if in 1981 the first two-temperature modeling of an arc plasma reactor was proposed [52]. However, over the past years there has been increasing evidence that the existence of LTE in thermal plasmas is rather the exception than the rule. Therefore, it was important to quantify the effects of deviations from LTE in order to provide guidance for computer simulation of flow, temperature, and particle concentrations in plasma reactors. This can only be achieved through a fundamental understanding of the basic phenomena

involved and their influence on the plasma properties, see for example [27, 52–61] among many other papers.

Plasma Spray Torches Used in Industry

Up to the nineties the most used plasma torches consist of a cathode and an anode arranged along a common axis. The cathode is usually a cone shaped rod of tungsten, which points at a hollow tubular copper anode ending in a nozzle [10, 62]. The plasma forming gas is injected along the cathode and the arc strikes between the cathode tip and the anode-nozzle serving as arc constrictor, Fig. 1. The arc is stabilized by the combination of the water-cooled cylindrical wall and the superimposed axial cold gas flow, especially when a swirl is used. The most used industrial plasma torches of this type are the Sulzer-Metco F4 and the Praxair SG 100 but power levels are generally below 50–60 kW. An important point is the long-term stability of the plasma jet and its influence on coating properties obtained when the torch working time increases.

The plasma jets obtained were rather different according to the plasma forming gas injection.

Heberlein [63] has identified the following types of voltage waveforms, reflecting three types of operating modes:

- the restrike mode (see principle in Fig. 1b) characterized by a saw-tooth voltage–time behavior and large voltage fluctuation amplitude, generally obtained with di-atomic gases,
- the takeover mode which has an approximately sinusoidal or triangular shape of the waveform with a relative low fluctuating amplitude and corresponding generally to mono-atomic gases,

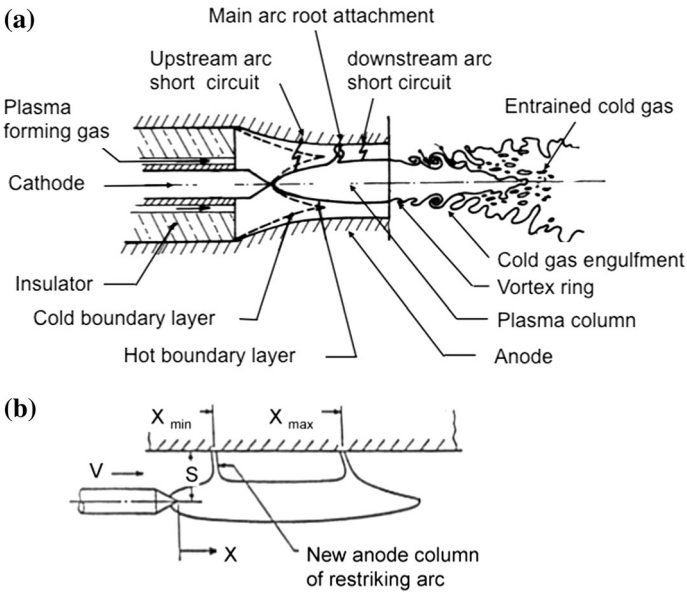

Fig. 1 Schematic representation of **a** an atmospheric pressure DC plasma-spraying torch [63], **b** of the restrike mode

- steady mode with an almost flat voltage profile but with very short electrode life (Fig. 2).

These different operating conditions depend mainly on the thickness of the relatively cold boundary layer between the arc column and the anode surface. This thickness is linked to the nozzle internal diameter, the arc current, the mass flow rate of the plasma-forming gas, and the vol% of diatomic gases.

Another point that must be considered is the electrode erosion, which can affect deeply the properties of the plasma jet and modify coating properties [56, 65].

The main developments of plasma torches were devoted to more stable arc voltage and reduction of electrodes wear, production of torches with higher powers and of torches permitting axial injection of particles. According to Marquès et al. [10] as early as 1964 one of first spray torch with more power and less fluctuations was that of Advanced Plasma Gun (APG) presented in Fig. 3. The arc channel consists of a number of water-cooled segments, electrically insulated from each other and from the anode (neutrodes) often called a cascaded arc.

With these torches, a much higher voltage between cathode and anode is obtained and limiting its axial movement to the anode length stabilizes the long arc. If at the anode, voltage fluctuations ΔV can reach 40–50 V with molecular gases, as the mean arc voltage V_m can be higher than 150 V, effects of fluctuations are drastically reduced. As the erosion of electrodes depends essentially on the arc current and fairly little on the voltage, power levels 3–4 times higher than with conventional torches can be achieved with of course longer plasma jets.

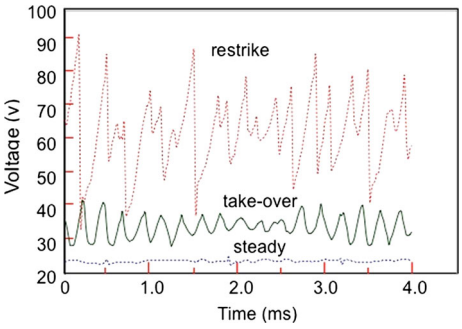

Fig. 2 Arc operating modes with 8 mm i.d. nozzle, Ar–He mixtures of plasma-forming gas and different arc currents [64]

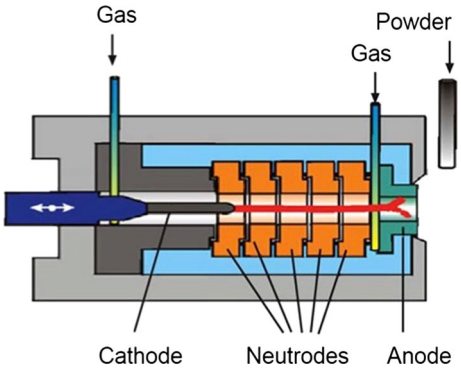

Fig. 3 Schematic of a plasma torch with neutrodes: advanced plasma gun (APG) [10]

Sulzer Metco, has presented in 1998 the Triplex torch where the arc current is divided into three separate arcs with three cathodes and one anode, but three separate anode attachments [66]. Neutrodes form the wall of the arcing channel. When observing the plasma jet for small anode-nozzle diameters, it can be observed that they are constituted of three lobes. Another plasma torch with neutrodes has been developed, 10HE High Enthalpy plasma torch [67]. Power levels can vary from 60 to 100 kW with plasma gas mixtures of Ar–N_2–H_2; e.g., 79.5 kW with arc current of 370 A and voltage of 215 V.

Another torch concept is that of Mettech Northwest corp., named Axial III torch, with the feedstock axial injection. It uses three plasma torches supplied by three independent power supplies. The feedstock is injected axially between the three plasma jets converging within an interchangeable water-cooled nozzle followed by an extension [68].

As pointed out by Marqués et al. [10] this concept of axial injection was probably introduced in 1985 with a Japanese patent application. Three individual cathodes were disposed around a water-cooled powder feeder tube, the common anode-nozzle having the same axis with the three arcs attaching to it. Thus injected powder travels in the core of the plasma jet exiting the nozzle. Marqués et al. [10] presented other configurations of the same type. Recently GTV GmbH in Germany has presented a commercial plasma torch with 3–5 anodes. It allows power levels up to 100 kW (current below 1000 A and voltage up to 120 V). We will not present plasma spray torches working at atmospheric pressure with water or argon and water, which applications are rather specific.

Plasma Jet Measurements

Salpeter [69] has developed in 1961 the theory of electron fluctuations in plasma and his work has permitted to develop measurements of temperature and density using Thomson laser scattering. For more details see Dzierżega et al. [70] and Shein et al. [71]. Thomson scattering is a local measurement, so it doesn't require rotational symmetry.

In most cases however plasma jet temperature measurements are based on emission spectroscopy of molecules ($T < 5000$ K), atoms (8000–14,000 K) and ions (over 14,000 K). Such measurements give the population of the emitting excited level [72–75] but assumptions must be made to deduce a temperature from this population. At equilibrium the volumetric emission coefficient, ε_λ, is calculated as a function of temperature for a given pressure. For plasma jet with a cylindrical symmetry the local value of ε_λ is obtained thanks to Abel's inversion [72–74]. Stark broadening, to determine the electrons density, does not impose any restrictions on the thermodynamic state (LTE) of the plasma [44, 45], but Abel's inversion is mandatory to obtain the radial distribution for the corresponding wavelengths of the line studied [74].

Measurements through absorption spectroscopy require using an emitting source that can be another plasma torch [75] for measurements in the plasma core or a hollow cathode lamp [76] in the plasma plume. Coherent Anti-Stokes Raman Spectroscopy (CARS) or Rayleigh scattering are also used, for $T < 8000$ K, CARS presenting high conversion efficiency [77]. All these measurements assume that the plasma is both, rotationally symmetric and optically thin.

Enthalpy probes were developed in 1962 [78]. They were used with Pitot probes to characterize plasmas jet plumes and the mixing of plasma with surrounding environment [79–81]. They were also coupled with a mass spectrometer to measure gas composition and

in 1993 an industrial probe was developed by Tekna Co. (Sherbrooke, Canada) to measure the plasma plume local enthalpy, temperature, velocity and composition.

Velocity measurements in the plasma jet core can be achieved by measuring the time of flight of the luminous fluctuations of the plasma supposed, to propagate at the flow velocity [82, 83]. It works especially well with restrike mode. Of course outside of the plasma core enthalpy probe can be used (temperatures below 6000–8000 K according to plasma gas) [79, 80].

Temperature measurements are more complex with torches such as the Triplex one, because the jet has no more axial symmetry. The emitted radiation of the plasma jet must be detected under several directions, one after the other and distributed over a sector of 180° in a plane perpendicular to the torch axis [81, 84, 85]. As in conventional emission spectroscopy, a cross-section of the plasma jet is imaged, through a lens system, on the entrance slit of the spectrometer and signals in its outlet plane are recorded through CCD camera. With non-symmetrical jet it is mandatory to detect, by a tomographic procedure, the emitted radiation under several angles of observation. The necessary conditions to apply this method are highly stationary plasma jets with a definite axis around which the total detecting optical system is rotated.

One must keep in mind that the response times of detection systems sometimes might be relatively long (milliseconds for example with CCD detectors) compared to arc voltage fluctuations in the 10^{-4} s time range (see Fig. 2). Thus the effect of voltage fluctuations is averaged.

At last visualization of plasma jets is important. It is achieved with photographs taken with a numerical camera and using different filters the picture being triggered for example by the arc voltage [2]. When injecting cold particles, cold gas or cold liquid a laser flashing can be used with a filter to eliminate part of the plasma signal. It permits to visualize the plasma and the injected droplets or particles to check the effect of the injection gas [2]. High-speed images of the luminous plasma jet for each operating condition can be acquired with a Laser-Strobe TM video camera, and the image analysis can be used to quantify the jet length and its fluctuations as additional torch responses [85].

As already pointed out, the voltage fluctuates (see Fig. 2) at frequencies of many kHz. As the current is constant, the instant dissipated power follows voltage frequencies. When spectroscopic measurements are performed using photomultipliers with response time in the microsecond range, the recorded signal fluctuates between those collected at the highest and lowest power. The question is which signal should be considered: that at the highest voltage, that at the lowest or that at the mean one. Temperatures, measured at a given point along the jet radius for a given axial distance, result from Abel's inversion. For example Fig. 4a presents the jet temperatures calculated with the highest values of the signal (upper part) and those calculated with the lowest values of the signal (lower part). Of course when using detectors with lower time response, a mean value between both is obtained. These results were obtained by assuming that in all type of measurements the jets keep their axial symmetry. Unfortunately it is far to be the case as shown in Fig. 4b. This figure was obtained with a camera at a frequency of 24 Hz and shutter time of 10^{-4} s. The obtained images are far to have an axial symmetry. This instability results from the constant movement of the arc root, as pointed out above, but also the extreme density and viscosity gradients between the low density, high viscosity plasma jet and the cold gas surroundings [86, 87].

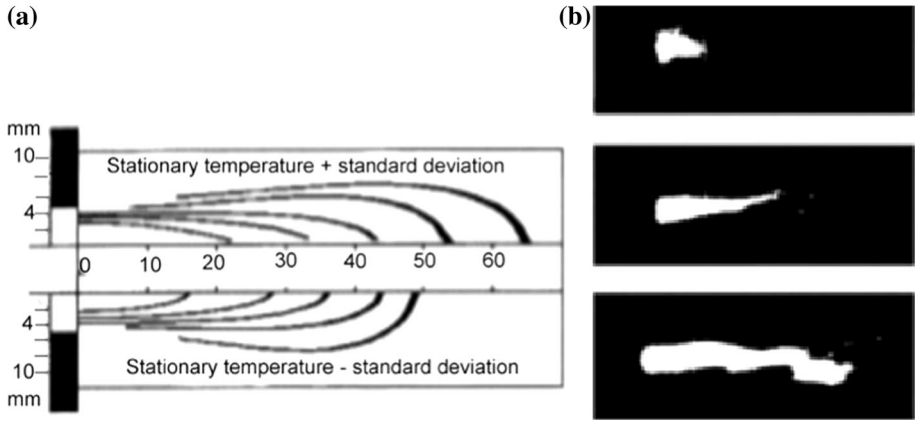

Fig. 4 **a** Temperature measured with photomultipliers with ArI 738.3 nm line ± standard deviation. Ar–H_2 (45–15 slm) plasma jet; nozzle i.d. 10 mm, I = 632 A, V = 61 V, thermal efficiency of the gun 56%, **b** pictures of a DC plasma jet taken with a shutter time of 10^{-4} s [87]

In-Flight Particles Measurements

In the seventies–eighties rather sophisticated measuring devices were used such as Laser Doppler Anemometry (LDA) for particle velocities and Phase Doppler Shift to also measure their diameters, fast (with response time as short as 100 ns) two-color pyrometers [72, 73], and also CCD cameras for the detection of the hot particle trajectories distribution within the plasma jet. The problem with pyrometers working with a unique wavelength is the necessity to know the corresponding emission coefficient. Particle temperature measurements can be disturbed due to signal absorption and light scattering by the plasma. However results are strongly linked to the calibration of devices [81, 87–89], and sensors developed at the end of nineties.

Phase-doppler anemometry (PDA) can also measure the particle flux density, which monitoring allows determining the optimal setting of spray parameters [90].

In the nineties, works showed that two types of measurements were possible: either a single particle technique, each particle being observed "one at a time" in a small volume (<1 mm^3) or ensemble of particles, observed at the same moment, in a long cylinder (more than the jet diameter) with a radius >1 mm. Industrial sensors, based on laboratory works, for example [91], were industrially developed [92]. These sensors are liable to work in the harsh environment of spray booths. The sensor, as soon as its weight is over 1 kg, is fixed aside the torch, which is moved regularly in front of it. A typical sensor for single particle technique is the DPV-2000 System (Tecnar Automation, Quebec, CN) measuring a single particle temperature, velocity and diameter. The latter is deduced from the signal emitted by the in-flight particle. However calculation results depend on measured temperature by the two-color pyrometer and the emission coefficient of the in-flight particle, often poorly known. Accuraspray®, also from Tecnar, is an ensemble measurement where the measuring volume is 25 mm long and 3 mm in diameter. Particle velocities are obtained from cross-correlation of signals, which are recorded at two closely spaced locations. The temperatures are determined by two-color pyrometry. A CCD camera enables the analysis of the plume appearance (position, width, distribution, intensity) along a line in spray distance perpendicular to the particle jet.

Figure 5 illustrates the difference of information obtained with both methods for YSZ particles. With DPV-2000 temperatures distribution is rather broad: from about 1000 °C (lower limit of such measurements) to 4000 °C and thus many particles are un-melted. The ensemble value, T_e, in Fig. 5 obtained with a Spray Watch (Oseir)sensor, is below the melting temperature T_m and seems reasonable, but is much less informative.

Mauer et al. [94] have also compared different measurements performed with both types of sensors. They found that results obtained with both systems were in good agreement, thus confirming the measurement accuracy of both. They showed that measurement of particle temperature close to plasma torch exit is generally more difficult to carry out by the Accuraspray-g3, which is probably due to the size of the measuring volume where plasma radiation is dominant relatively to the particle radiation.

The power fluctuations have also an important effect on the injected particles [95]. This is obvious when considering the series of high-speed images in Fig. 6 [95].

These fluctuations lead to uneven particle heating. Furthermore, they lead to the entrainment of cold surrounding gas in the jet, rapidly reducing its average temperature and velocity. Particle velocity measurements show that particles injected inside the nozzle have consistently much higher velocities than those injected outside the nozzle. This due to the fact that particles injected outside the nozzle are entrained in cold gas bubbles which reach the nozzle axis, but do not break up until several nozzle diameters downstream from the nozzle exit [95]. However most models assume that the plasma jet has an axial symmetry and that its velocities and temperatures are those corresponding to the mean voltage (mean values between those presented in Fig. 4a).

The penetration of particles within the plasma jet has been extensively studied since the eighties. At that period the problem was to follow the in-flight particle temperatures and velocities in the plasma jet. The powder was sieved in narrow distributions (d ± 2 or 3 μm). For different sizes with very low particle flow rates, the in-flight particle position was determined and its temperature (fast pyrometry) and velocity (laser doppler anemometry) measured. An example of such measurements [96] is presented in Fig. 7. The optimum injection velocity is 25 m/s. The optimum injection velocities were determined for particles with different sizes distribution: 25 m/s for 18 μm, 22 m/s for 23 μm, 18 m/s for 39 μm, and 14 m/s for 46 μm particles and also different materials.

Beside the choice of particles size distribution and morphologies their injection [96] is a complex process, which also plays a key role in the properties of resulting coatings [97],

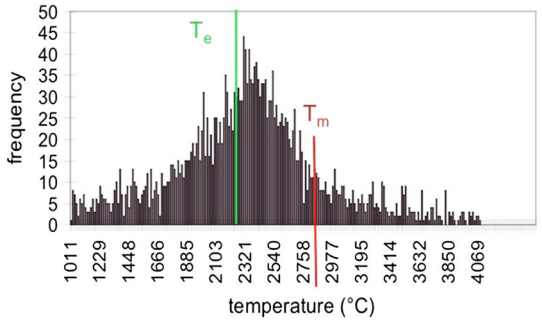

Fig. 5 In-flight temperatures distribution of yttria-stabilized-zirconia (YSZ) particles (fused and crushed, 5 and 22 μm) sprayed in soft vacuum with a PTF4 torch, laval nozzle, Ar–H_2 mixture (40–6 slm), 750 A, and measurements performed with a DPV2000 (statistical distribution) and a spray watch (ensemble value T_E). The melting temperature, T_m, is indicated [93]

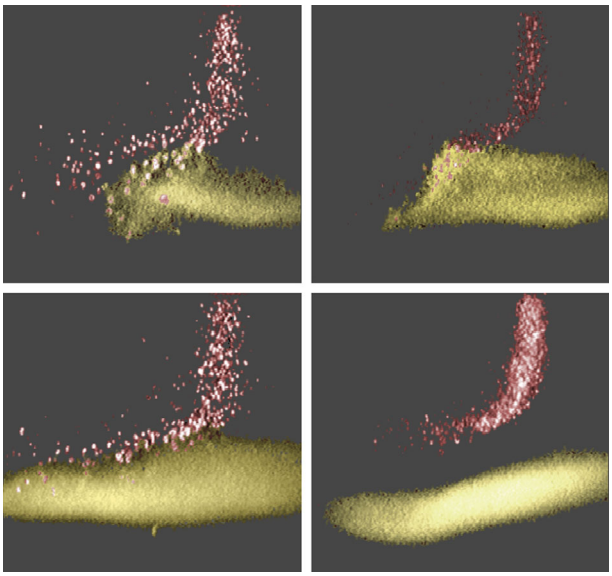

Fig. 6 High speed images showing the fluctuations of the plasma jet and the spray particle fluxes being exposed to varying environments [95]

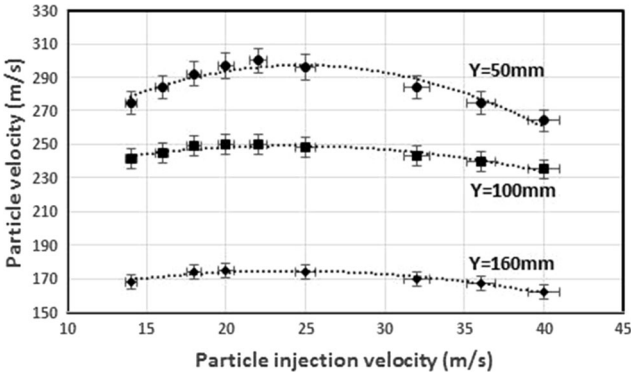

Fig. 7 Experimental velocity of alumina particles (18 ± 2 μm in diameter) versus injection velocity in nitrogen–hydrogen plasma (29 kW, N_2 37 slm, H_2 27 slm, anode-nozzle i.d. 6 mm). Measurement performed at different distances, Y, from nozzle exit [96]

especially for radial injection. Particle penetration in the jet depends on: the injector internal diameter and shape (straight or curved), its position and inclination relatively to the plasma jet for external injection, while internal injection can induce a high deviation of the plasma jet as soon as the carrier gas exceeds 10% of the plasma mass flow rate [97]. An important problem is linked to the particles bypassing the plasma jet and entrained in its fringes, but heated enough to stick on the coating under formation.

The sensor spray and deposit control (SDC®) fixed on the plasma torch [92], uses either a CCD camera or a photodiode array where the image of a section of the plasma jet plume or the core is focused. A filter with a 3 nm band pass allows eliminating the most important part of the plasma plume light. As illustrated already for particles with very narrow size

distribution in Fig. 7 the particle injection velocity, controlled by the injector internal diameter and carrier gas flow rate, plays a key role in particle trajectories. In Fig. 8a are presented schematically the different mean trajectories of particles depending on the carrier gas flow rates. In Fig. 8b for alumina particles the SDC sensor records the corresponding light intensities for different carrier gases. The maxima observed for the different carrier gas flow rates are shifted to the right or the left of the optimal one (corresponding for these spray conditions to an argon carrier gas flow rate of 4.5 slm).

Plasma Jets and Plasma Torches Modeling

First it is important to keep in mind that the modeling is not only performed to characterize the plasma within the anode nozzle, but essentially the plasma jet issued from the torch and its interaction with the particles injected [98, 99]. In one of the first models developed [100] the following assumptions used were: LTE, symmetrical arc about torch axis (2D equations), arc optically thin, turbulent and an isotropic flow but spatially variable eddy, negligible compressibility effects, no density fluctuations due to turbulence, constant specific heat (oversimplified) and given temperature and velocity profiles at nozzle exit with an internal radius r_n for example by:

$$A(r) = A_{max}[1 - (r/r_n)^n] \quad \text{where} \quad A \text{ is } T \quad \text{or} \quad v$$

The values of T_{max}, v_{max} and n must be carefully determined to cope with experimental results. For example in this early model the theoretical predictions were in good agreement with the experimental measurements regarding the behavior of nitrogen plasma discharging into air. However the agreement was less satisfactory with respect to argon plasma discharging into air, particularly as far as the temperatures were concerned, in the low-temperature range.

Legros [100] performed calculations for the plasma jet where temperature and velocity radial distributions were measured values. The turbulent energy dissipation was calculated through a mixing length, model called (V&T). The second calculation was based on the

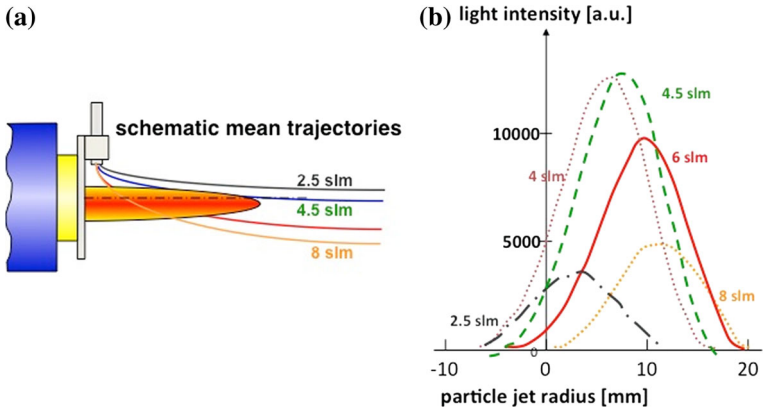

Fig. 8 SDC measurement of alumina particles heat flux 60 mm downstream of the nozzle exit of an Ar–H_2 plasma (45 slm Ar, 15 slm H_2, 6 mm i.d., Peff = 20 kW, injector i.d. = 1.75 mm, disposed 3 mm downstream of the nozzle exit and at 8 mm from the torch axis) with different argon carrier gas flow rates. Effects on particles: **a** mean trajectories, **b** radial distribution of emitted light intensity [97]

dissipation of the electrical energy modeled in a cylindrical volume V_m located in the cylindrical anode, assumed to be a heat source with a uniform volume heat (W/m^3) defined as $V.I/V_m$, model called (PV). Typical results are presented in Fig. 9 for an Ar–H_2 plasma jet flowing in air.

Plasma jets modeling is complex for different reasons:

- When the plasma jet leaves the nozzle, it encounters a steep laminar shear at the outer edge of the jet as shown by Pfender [101, 102]. The large velocity difference results in the rolling up of the shear at the outer edge of the jet around the nozzle exit into a ring vortex. As shown in Fig. 1, this vortex is pulled downstream with the flow and thus the process repeats itself again at the nozzle exit. The formed vortex rings at the outer edge of the jet have the tendency to coalesce, forming larger vortices with wave instabilities growing around the entire ring. It results in large-scale engulfment of external surrounding gas (mostly air). These large eddies, at low temperature, have a high inertia, are heated progressively, and break in smaller eddies that can diffuse in the plasma jet. By seeding micrometer sized oxide particles either in the plasma jet or in its surrounding and measuring their velocities, Pfender et al. [101] showed that for an argon plasma jet, the plasma fluid has a much higher mean velocity than the entrained gas reaching the torch axis. Such results help understanding why the same plasma jet core is longer when flowing in argon atmosphere ($p = 10^5$ Pa) than in air [103], a nitrogen atmosphere giving a length between both.
- Huang et al. [104] introduced a two-fluid turbulence model for predicting the conditional flow properties of the turbulent plasma jet. The model was able to predict phenomena not taken into account in more conventional models.
- Realistic models for spray torches with single cathode and anode (single-arc systems) should be three-dimensional to enable taking into consideration the transverse injection of a cold gas [105, 106], the arc unsteady attachment at the anode [105–109], the three-dimensional character of turbulence structures [110, 111] and cold gas entrainment [109].
- However different turbulent models exist and authors recommend that the use of turbulence models of the flow in DC arc torches is approached with care and weighting the assumptions and approximations involved.

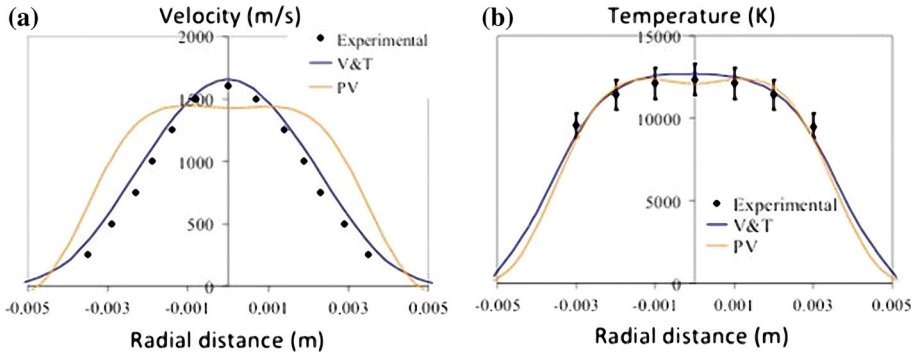

Fig. 9 In a plane 2 mm downstream of the nozzle exit, radial profiles of the calculated and measured plasma flow, **a** velocity, **b** temperature. Plasma jet produced by a torch with an anode-nozzle 7 mm in i.d., Ar 45 slm, H_2 15 slm, 600 A, 65 V, thermal efficiency 55%, flowing in air at atmospheric pressure [100]

- In fact, coupling the electromagnetic and heat transfer phenomena in a non-transferred arc plasma torch should be determined. It requires coupling the electromagnetism and energy conservation equations for the fluid and the electrodes [112].
- The flow pattern of a plasma jet with superimposed vortex flow differs substantially from its counterpart of a uniform cold flow jet [113].
- The interactions of the plasma jet with the substrate depending on the distance nozzle exit-substrate orthogonal to plasma jet axis [114], as well as its inclination [115] or shape [116] are not negligible.
- The mixing of the high velocity and turbulent plasma jet can be improved by using especially designed nozzles positioned at the cylindrical anode-nozzle exit [117, 118].
- Compressible effects should be considered for spray torches working in air atmosphere with nozzles to produce supersonic plasma jets where velocities are up to 2200 m/s with sound velocity of about 3000 m/s.
- At last close to walls or electrodes, non-equilibrium should be considered, as well as chemical non-equilibrium with corresponding data banks [119].
- The development and use of plasma torches with cathodes or anodes and often neutrodes is linked to their advantages erosion, higher particle velocities, and better deposition efficiency. Thus models should be developed. Bobzin et Öte [120] were among the firsts to develop such models.

Modeling Heat and Momentum Transfer to Particles

Single Particle

Plasma spraying requires the proper control of particle trajectories, on which depend their temperature and momentum histories. In fact a slight deviation from near optimal conditions, can easily lead to poor results due to either the lack of melting of particles, or the modification of their composition due to particle evaporation. In the eighties and nineties most papers on this topic were published [87, 121–129].

Beside the bases of momentum and heat transfer to a single particle, generally spherical, one must consider corrections due to temperature gradients and non-continuum effects. Attention must also be given to internal heat conduction in the particle and heat losses due to the particle radiation. Also the particle composition modifications, must be considered, with successively:

- The evaporation of the particle: evaporation rate, heating of the vapor and vapor buffer effect on heat transfer and radiation of the vapor,
- The non-isotherm behavior, particle shape and particle charge,
- The particle reaction with its surrounding: reaction with the vapor or the solid or liquid particle.

Momentum Transfer

For the momentum transfer, the drag coefficient C_D is expressed as a function of the Reynolds number Re of the particle, but different expressions exist according to the values of Re [125, 130–134]. The corrections due to temperature gradients are not negligible and the particle trajectory can be modified [126]. The effect of non-continuum or Knudsen, Kn,

effect is also important in the range $10^{-2} < \mathrm{Kn} < 1$ [135–137]. An example of results is presented in Fig. 10. A 20 μm diameter alumina particles was chosen because of its a significant non-continuum effect and was injected at 25 m/s in the plasma jet ($Ar–H_2$, 75–15 slm, P = 29 kW, ρ_{th} = 63%, nozzle i.d. 8 mm). Here again the different types of corrections used have an important effect on the calculated particle trajectory and particle velocity and temperature.

The effect of turbulence on the particle motion, as illustrated in Fig. 11, can also have an important influence especially for small particle trajectories [125]. For example turbulence is not negligible for particles, 10–50 μm, injected into argon DC turbulent plasma jet.

The shape of the particle modifies its drag coefficient [135], correlated to the particle sphericity. However when injected into the plasma, particles are rapidly (∼a few tens of

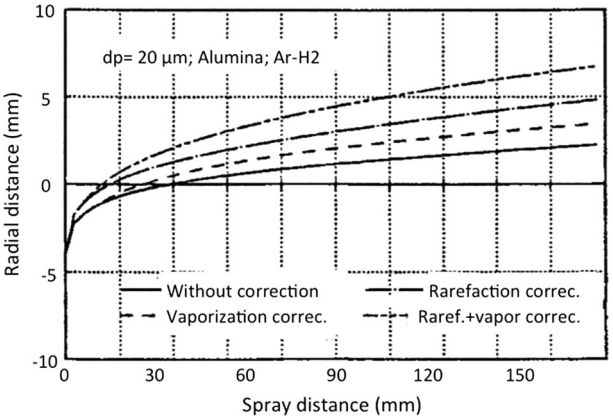

Fig. 10 Trajectories of 20 μm in diameter alumina particles injected at 25 m/s into the plasma jet depicted in Fig. 11 (radial distance = 0 corresponds to the torch axis). The temperature gradient correction has been calculated using the mean integrated properties [136]

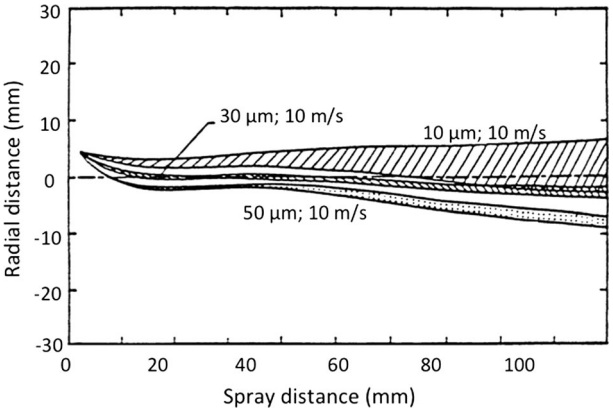

Fig. 11 Dispersed alumina particle (10, 30, 50 μm) trajectories in argon DC turbulent plasma jet [125]

μs) heated above or close to their melting point, thus attaining a spherical shape. Non-sphericity effect plays a role mainly close to the injector.

The particle charging has a limited effect [121, 126] because of the low charge concentration that can exist in the region near the particle surface.

At last the arc root fluctuations, especially in the restrike mode, modify particle trajectories according to different instants of fluctuations [121]. The synchronization of the DPV2000 sensor with voltage fluctuations allowed measuring particle parameters as functions of the time delay. For alumina particles, the periodic variations of temperature were about 500 °C and velocity around 200 m/s, as illustrated in Fig. 12. In this case, the effective power varies between 12 and 35 kW! The period of the cycles coincides with that of voltage fluctuations (period 220 μs or f = 4500 Hz). This is due to the particle momentum with respect to the instantaneous momentum of the gas at the point where the particle penetrates the jet flow [106, 138].

Heat Transfer

The balance between conduction and convection heat transfers from the hot gas to the particle, are generally neglected [26] and particle cooling due to radiative heat losses to the surroundings governs the particle temperature. The heat transfer coefficient, h, between plasma and particle can be expressed in terms of the Nusselt number Nu, linked to the numbers of Reynolds, Re, and Prandlt, Pr. Authors [106, 126, 134, 139–142] have proposed different expressions of Nu and thus of h. Differences are particularly important when considering diatomic gases such as Ar–H_2. This is illustrated in Fig. 13 representing the calculated [126] heat transfer coefficients versus temperature for a stainless steel 50 μm particle, at T_p = 1000 K, and traveling at 50 m/s.

The heat transfer, Q, to the particle is calculated according to the hot gas temperature T_∞ "seen" by the particle along its trajectory, which has to be calculated first. Of course, beside its chemical composition, the particle morphology, depending strongly on its manufacturing process [147], plays a key role in its thermal conductivity κ_p. The radiative losses from particles increase with their size but their influence on the particle temperature is more pronounced when the size of the particle is small (higher surface/volume ratio).

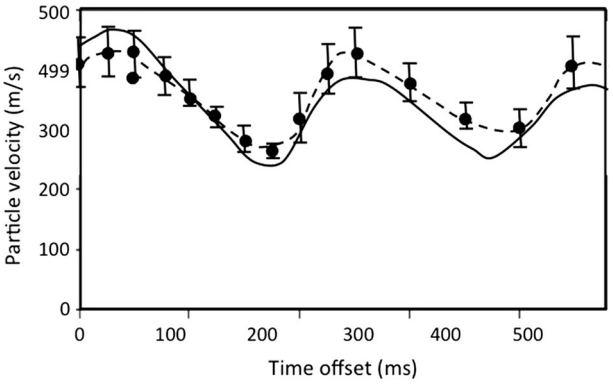

Fig. 12 Calculated [106] (continuous line) time dependence of the velocity of alumina particles (5–45 μm) in a fluctuating Ar–H_2 DC. plasma jet (nozzle i.d. 7 mm, Ar 35 slm, H_2 10 slm, I = 550 A, P_{eff} = 19.25 kW). Measurements points taken 50 mm downstream from the nozzle exit on the jet axis [138]

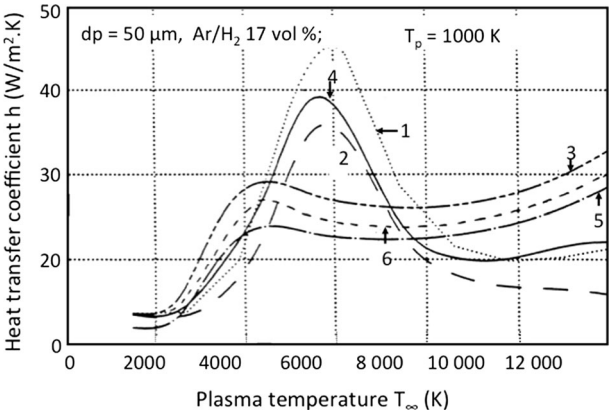

Fig. 13 Heat transfer coefficient for a 50 µm diameter stainless steel particle travelling at 50 m/s with $T_p = 1000$ K in Ar–H_2 (17 vol%) plasma according to (1) [134] (2)—[143], (3) convection and conduction calculated with integrated properties [144], (4) [145], (5) Nu = 2 [142], (6) [146]

The easiest for calculations is to assume a uniform temperature, implying that the Biot number, $Bi = \kappa/\kappa_p$, is <0.01 where κ is the plasma thermal conductivity. It occurs if $\kappa \gg \kappa_p$ i.e. if the particle thermal conductivity, κ_p, is high.

The particle transient heating, especially when its thermal conductivity is low must also be taken into account.

The porosity of particles, for example of agglomerated ones, can reduce their thermal conductivity [148].

The non-continuum effect in plasma-particle heat transfer over the same Knudsen number range ($0.01 < Kn < 1.0$) is important [149].

Hot gas–particle heat transfer becomes much more complex in the presence of simultaneous mass transfer, such as particle vaporization, modifying the heat transfer through the vapor layer created around the particle. Moreover, the radiation from the vapor cloud surrounding is generally much higher than that of the plasma gas. The mass transfer and evaporation rate of the particle will depend, on the vapor diffusion within the boundary layer provided that the saturation pressure of the vapor p_s is lower than that of the surrounding atmosphere. The complexities of the calculations increase substantially.

During the evaporation of metallic particles, radiative energy losses from the metal vapor cloud surrounding the particle cannot be neglected in contrast to that of the plasma [47, 150]. The presence of a reactive gas in the atmosphere around liquid particles may also affect their vaporization.

In plasma jets the velocity difference between the molten particle in flight and the gas flow can induce a convective motion within the droplet. When the ratio of the kinematics viscosities of the plasma and the droplet is higher than 50, and the Reynolds number of the flow relative to droplet higher than 20, a convective phenomenon is induced within the droplet [151]. Therefore, the presence of a flow-induced vortex in the molten particle can be expected [151]. The recirculating flow within the droplet results in an increase of the oxygen content compared to that estimated assuming a pure diffusion model [152]. For example in liquid Fe particle, the Fe_xO drops entrained by convection are not miscible and upon cooling both phases, separate and spherical Fe_xO_y nodules are formed within the solidified particle as shown in Fig. 14 with 15 wt%, while diffusion calculations estimate the Fe_xO_y concentrations to be less than 3 wt%.

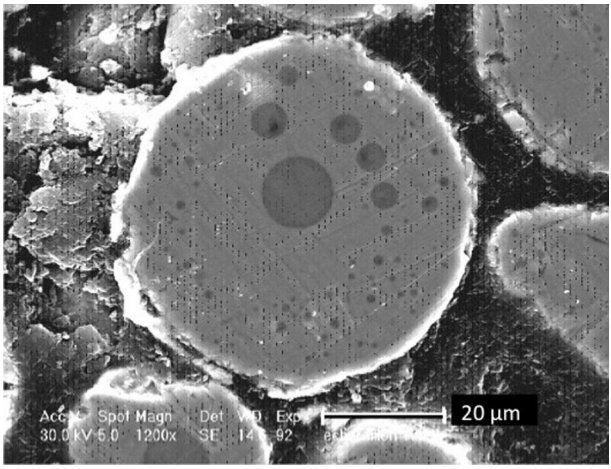

Fig. 14 Cross sections of a low carbon steel particle collected at z = 100 mm after its flight in a D.C. plasma jet: Ar 50 slm, H_2 10 slm, I = 500 A, nozzle i.d. 7 mm. SEM analysis at 30 keV [152]

Similar results were obtained with stainless steel [153].

As the particle injection rate increases, particles start to alter the plasma properties significantly, phenomenon called "particle loading of the plasma". The effect is due to the heat transfer to particles but also, when spraying materials evaporating very fast, to the increase of radiative emission. This effect has been more studied for RF plasmas than for DC ones [154].

Of course all phenomena presented above about momentum and heat transfers depend strongly of the plasma jet produced [155].

Splats Formation and Layering

To achieve a coating many particles are injected per second with the resulting splats formation and layering. According to the present knowledge, nobody has a clear idea of the effect on coating thermo-mechanical and service properties of the impact, flattening, solidification and layering of particles.

First a better understanding of splat formation (flattening in a few µs) is the base of the coating formation control according to the reviews published in 2004 and 2009 [156–158]. Unfortunately actually no camera can follow this flattening.

Most of recent works were performed through high speed imaging by photographing one single particle during its flattening in a given time range [159–163]. When varying the time range for different particles, assumed to be identical at impact (same diameter, temperature and velocity), it becomes possible to obtain few photographs (less than ten) of the flattening at different times. These measurements have confirmed the drastic influence of the flattening velocity in the splat formation; velocity linked to impact parameters and substrate properties such as cleanliness and oxide layer at surface of metals or alloys. However according to available optic depth of field, these studies were only possible on smooth substrates [161–163]. They have demonstrated the importance of substrate pre-heating, just prior spraying, over the so-called transition temperature, T_t, [156, 157] to get rid of adsorbates and condensates. On these hot surfaces, almost disk shaped splats are

obtained. Coating adhesion depends strongly on substrate preheating over T_t and its roughening adapted to the mean size of impacting temperature. The adhesion of the same coating deposited on the same cold or hot (preheated over T_t) substrate is up to 10 times higher. The mechanical adhesion between the splat and substrate asperities depends on its size compared to that of the surface peaks, which can be characterized by their R_t (distance between their highest peak and deepest under cut). Roughly, for a good adhesion, the splat mean diameter must be between 1.5 and 3 times R_t. Bahbou and Nylen [164] have studied the influence of the different roughness parameters: R_a, R_t,R_{sm} and $R_{\Delta q}$ on the adhesion of Ni–Al (5 wt%) coating plasma sprayed onto Ti6Al4 V grit blasted substrates,. Results show that the adhesion values measured are poorly correlated with R_a or R_{sm}. However the surface peak is not sufficient and the liquid must penetrate into the cavities, requiring that the impact pressure is high enough [165].

Of course the coating adhesion is reduced if many unmelted small particles are trapped in the coating. It demonstrates that the particles size distribution choice and their injection according to the plasma jet is also one of the key parameters. Particles travelling in the plasma jet fringes and heated enough to stick to bead wings are also responsible of important adhesion defects in the pass resulting of beads overlapping.

It must be pointed out that besides all the works in laboratories, the industrial developments of plasma sprayed coatings has also been boosted for:

- the industrial adapted spray booths [160],
- the constant evolution of control panels [1, 7], connected, through computers, to the different equipment's, including, since the beginning of the new millennium, sensors following in-flight particles,
- the development of robots with computer-aided trajectory to manufacture coatings on complex geometries requiring optimized torch movement [1, 7].

The characterization of coating microstructures and properties has also been considerably developed. However works are still mandatories to achieve a better understanding of coatings generation. Another topic, which has been approached but not developed, should be the study of the crystal structure adaptation between the bond coat and the coating.

Conclusions

During almost sixty years plasma spraying progressively became a science. This is due to different factors:

- Up to the nineties the understanding of which parameters control plasma jets obtained with plasma torches where the cathode and anode were arranged along a common axis (conventional torches). This has been performed thanks to plasma thermodynamic and transport properties calculations, modeling first of plasma jets and later the plasma behavior inside the torch, the entrainment of the surrounding atmosphere, comparison of different model results with measurements and visualizations of the plasma jet. In parallel new plasma torches with cathodes or anodes or both, some of them including neutrodes were developed to achieve less electrode erosion and higher power levels as well as longer plasma jet cores (where temperature >8000 K). Moreover these torches have lower arc fluctuations, compared to conventional ones
- The modeling and measurement of in flight particles and their injection. These works have resulted in the development of sensors able to work in the harsh environment of

spray booths allowing controls in industrial conditions, achieved up to the mid-nineties in laboratories.

- Coating quality improvement was also boosted by the industrial development of:

… More sophisticated control panels of spray process,

… Optimized torch movement boosted by the development of robots with computer-aided trajectory,

- We must also point out that since the beginning of the millennium numerous works (about 30 to 40% of plasma spray papers) [13, 14] were devoted to suspension and solution spraying, but it was not the subject of this paper.

References

1. Tucker RC Jr (ed) (2013) Thermal spray technology vol 5A. ASM Int. Handbook
2. Fauchais P, Heberlein J, Boulos M (2014) Thermal spray thermal spray fundamentals. Springer, Berlin, p 1550
3. Muehlberger E (1988) Industrial plasma processing technology. In: Proc. 1st plasma technik symp, vol 3. Plasma Technik, Wohlen, pp 105–118
4. Freslon A (1995) Plasma spraying at controlled temperature and atmosphere. In: Berndt CC, Sampath S (eds) Thermal spray: science and technology. ASM Int., OH, pp 57–63
5. Ambühl P, Meyer P (1999) Thermal coating technology in controlled atmospheres (ChamProTM). In: Lugscheider E, Kammer PA (eds) Proceedings of the ITSC. DVS, Düsseldorf, pp 291–92
6. Friis M, Persson C (2003) Control of thermal spray processes by means of process maps and process windows. J Therm Spray Technol 12(1):44–52
7. Davis JR (ed) (2004) Handbook of thermal spray technology. ASM Int., Materials Park
8. Smith RW (1991) Plasma processing… the state of the art… and future—from a surface to a materials processing technology, 2nd Plasma-Technik- Symposium vol 1. Plasma-Technik AG, Wolhen, pp 17–38
9. Dzulko H, Forster G, Landes KD, Zierhut J, Nassenstein K (2005) Plasma torch developments. In; Proc. intern. thermal spray conf., DVS, Basel
10. Marqués J-L, Forster G, Schein J (2009) Multi-electrode plasma torches: motivation for development and current state-of-the-art. Open Plasma Phys J 2:89–98
11. Sun X, Heberlein J (2005) Fluid dynamic effects on plasma torch anode erosion. J. Therm Spray Technol 14(1):39–44 **(Page 25 of 53 26)**
12. Zhou XJ, Heberlein J (1994) Arc cathode erosion studies. In: Fauchais P (ed) Proc. of plasma symposium on heat and mass transfer under plasma conditions. Begell House Inc. New York, pp 237–243
13. Killinger A, Gadow R, Mauer G, Guignard A, Vaßen R, Stöver D (2011) Review of new developments in suspension and solution precursor thermal spray processes. J Therm Spray Technol 20(4):680–695
14. Fauchais P, Joulia A, Goutier S, Chazelas C, Vardelle M, Vardelle A, Rossignol S (2013) Suspension and solution plasma spraying. J Phys D: Appl Phys 46:224015
15. Fowler FH, Guggenheim EA (1956) Statistical thermodynamics. University Press, Cambridge
16. Glouchko VP (1962) Propriétés thermodynamiques des corps purs. Mir, Moscou
17. JANAF (1971) 'Thermochemical data' compiled and calculated by the Dow Chemical Company. Thermal Laboratory, Midland
18. Gordon S , Mcbride BJ (1994) Computer program for calculation of complex chemical equilibrium compositions and applications' NASA Report RP-1311. NASA Lewis Research Center, Washington, DC
19. Barin I, Knacke O (1973–1977) Thermochemical properties of inorganic substances. Springer, Berlin
20. Fauchais P, Baronnet JM, Bayard S (1975) Problèmes posés par le calcul des fonctions de partition des espèces mono et diatomiques dans un plasma. Rev Int Hautes Temp Réfract 12:221–232
21. Fauchais P, Vasseur A, Manson N (1969) Détermination des caractéristiques thermodynamiques des plasmas de mélanges de gaz. Rev Int Hautes Temp Réfract 6:5–20
22. Drellishak KS (1963) Partition functions and thermodynamic properties of high temperature gases. PhD thesis, Northwestern University

23. Capitelli M, Ficocelli E, Molinari E (1969) Equilibrium compositions and thermodynamic properties of mixed plasmas I, He–N2, Ar–N_2, Page 26 of 53 and Xe–Ne plasmas at one atmosphere between 5000 K and 35000 K, internal report, Univ. of Bari, Italy
24. Pateyron B, Elchinger M-F, Delluc G, Fauchais P (1992) Thermodynamic and transport properties of Ar–H_2 and Ar–He plasma gases used for spraying at atmospheric pressure. I: properties of the mixtures. Plasma Chem Plasma Process 12(4):421–448
25. Pateyron B, Aubreton J, Elchinger MF, Delluc G, Fauchais P (1986) Thermodynamic and transport properties of N2, 02, H2, Ar, He and their mixtures. Internal report, Laboratoire Céramiques Nouvelles URA 320 CNRS, University of Limoges
26. Boulos MI, Fauchais P, Pfender E (1994) Thermal plasmas, fundamentals and applications. Plenum Press, New York, p 448
27. Krenek P (2008) Thermophysical properties of H2O–Ar plasmas at temperatures 400–50,000 K and pressure 0.1 MPa. Plasma Chem Plasma Process 28:107–122
28. Mostaghimi-Tehrani J, Pfender E (1984) Effects of metallic vapor on the properties of an argon arc plasma. Plasma Chem Plasma Process 4(2):129–139
29. Pateyron B, Elchinger MF, Delluc G, Fauchais P (1996) Sound velocity in different reacting thermal plasma systems. Plasma Chem Plasma Process 16(1):39–57
30. Chapman S, Cowling T (1952) The mathematical theory of non-uniform gases. Cambridge University Press, New York
31. Hirschfelder JO, Curtiss CF, Bird RB (1964) Molecular theory of gases and liquids, 2nd edn. Wiley, New York
32. Butler JN, Brokaw RS (1957) Thermal conductivity of gas mixtures in chemical equilibrium. J Chem Phys 26:1636–1642
33. Aubreton J, Elchinger MF, Andre P (2013) Influence of partition function and interaction potential on transport properties of thermal plasmas. Plasma Chem Plasma Process 33:367–399
34. Gleizes A, Gonzalez JJ, Freton P (2005) Topical review, thermal plasma modeling. J Phys D Appl Phys 38:R153–R183
35. Murphy AB, Arundell CJ (1994) Transport coefficients of argon, nitrogen, oxygen, argon-nitrogen, and argon-oxygen plasmas. Plasma Chem Plasma Process 14(4):451–490
36. Devoto RS (1968) Transport coefficients of partially ionized hydrogen. J Plasma Phys 2(4):617–631
37. Aubreton J, Elchinger MF, Vinson JM (2009) Transport coefficients in water plasma: part I: equilibrium plasma. Plasma Chem Plasma Process 29:149–171
38. Murphy AB (2012) Transport coefficients of plasmas in mixtures of nitrogen and hydrogen. Chem Phys 398:64–72
39. Murphy AB (2000) Transport coefficients of hydrogen and argon–hydrogen plasmas. Plasma Chem Plasma Process 20(3):279–297
40. Pateyron B, Elchinger MF, Delluc G, Fauchais P (1990), Thermodynamic and transport properties of air and air–Cu at atmospheric pressure. Internal report, LMCTS, University of Limoges
41. Murphy AB, Tanaka M, Yamamoto K, Tashiro S, Sato T, Lowke JJ (2009) Review article, modelling of thermal plasmas for arc welding: the role of the shielding gas properties and of metal vapour. J Phys D: Appl Phys 42:194006
42. Gleizes A, Cressault Y, Teulet Ph (2010) Mixing rules for thermal plasma properties in mixtures of argon, air and metallic vapors. Plasma Sour Sci Technol 19:055013
43. Cressault Y, Gleizes A (2010) Calculation of diffusion coefficients in air–metal thermal plasmas. J Phys D: Appl Phys 43:434006
44. Griem H (1964) Plasma spectroscopy. McGraw-Hill, New York
45. Griem H (1974) Spectral broadening by plasma. Academic, New York
46. Cabannes F, Chapelle J (1971) Reactions under plasma conditions chapter 7. In: Spectroscopic plasma diagnostic, vol 1. Wiley, New York
47. Essoltani A, Proulx P, Boulos MI, Gleizes A (1990) Radiation and self—absorption in argon–iron plasmas at atmospheric-pressure. J Anal At Spectrom 5:543–547
48. Essoltani A, Proulx P, Boulos MI, Gleizes A (1994) Effect of the presence of iron vapors on the volumetric emission of Ar/Fe and Ar/Fe/H2 plasmas. Plasma Chem Plasma Process 14:301–315
49. Essoltani A, Proulx P, Boulos MI, Gleizes A (1994) Volumetric emission of argon plasmas in the presence of vapors of Fe, Si and Al. Plasma Chem Plasma Process 14:437–450
50. Rahmani B (1989) Calcul de l'émission nette du rayonnement des arcs dans SF6 et dans les mélanges SF_6–N_2, Engineering PhD, Univ. of Toulouse (in French)
51. Cressault Y, Rouffet ME, Gleizes A, Meillot E (2010) Net emission of Ar–H_2–He thermal plasmas at atmospheric pressure. J Phys D Appl Phys 43:335204

52. Chen DM, Hsu KC, Pfender E (1981) Two-temperature modeling of an arc plasma reactor. Plasma Chem Plasma Process 1:295–314
53. Aubreton J, Elchinger MF, Fauchais P (1998) New method to calculate thermodynamic and transport properties of a multi-temperature plasma: application to N_2 plasma. Plasma Chem Plasma Process 18(1):1–27
54. André P, Aubreton J, Elchinger MF, Fauchais P, Lefort A (1999) Plasma concentrations out of equilibrium: N_2 (kinetic method and mass action law), Ar–CCl4 and Ar–H_2CCl4 (mass action law). In: Fauchais P, Amouroux J (eds) The annals of the New York Academy of Sciences, New York, pp 85–94
55. Rat V, André P, Aubreton J, Elchinger MF, Fauchais P, Lefort A (2002) Two-temperature transport coefficients in argon–hydrogen plasmas—II: inelastic processes and influence of composition. Plasma Chem Plasma Process 22(4):475–493
56. Ghorui S, Heberlein JVR, Pfender E (2007) Thermodynamic and transport properties of two-temperature oxygen plasmas. Plasma Chem Plasma Process 27:267–291
57. Colombo V, Ghedini E, Sanibondi P (2009) Two-temperature thermodynamic and transport properties of argon–hydrogen and nitrogen–hydrogen plasmas. J Phys D Appl Phys 42:055213
58. Ghorui S, Heberlein JVR, Pfender E (2008) Thermodynamic and transport properties of two-temperature nitrogen–oxygen plasma. Plasma Chem Plasma Process 28:553–582
59. Meher KC, Tiwari N, Ghorui S (2015) Thermodynamic and transport properties of nitrogen plasma under thermal equilibrium and non-equilibrium conditions. Plasma Chem Plasma Process 35:605–637
60. Meher KC, Tiwari N, Ghorui S, Das AK (2014) Multi-component diffusion coefficients in nitrogen plasma under thermal equilibrium and nonequilibrium conditions. Plasma Chem Plasma Process 34:949–974
61. Yang A, Liu Y, Zhong L, Wang X, Niu C, Rong M, Han G, Zhang Y, Lu Y, Wu Y (2016) Thermodynamic properties and transport coefficients of CO_2–Cu thermal plasmas. Plasma Chem Plasma Process 36:1141–1160
62. Fauchais P, Vardelle A (1997) Thermal plasmas. IEEE Trans Plasma Sci 25(6):1258–1280
63. Heberlein J (2000) Electrode phenomena in plasma torches. In Fauchais P, Heberlein J, van der Mullen J (eds) Heat and mass transfer under plasma conditions. Annals of New York Academy of Sciences, pp 14–27
64. Duan Z, Heberlein J (2002) Arc instabilities in a plasma spray torch. J Therm Spray Technol 11(1):44–51
65. Leblanc L, Moreau C (2001) The long-term stability of plasma spraying. J Therm Spray Technol 11(3):380–386
66. Zierhut J, Haslbeck P, Landes KD, Muller BGM and Schutz M (1998) TRIPLEX—an innovative three-cathode plasma torch. In: Coddet C (ed) Proc. proc. intern. thermal spray conf. ASM International Materials Park, Nice, pp 1374–1380
67. Sahoo P (2006) 100HETM plasma spray system. Patent US 20060099440 A1
68. Oberste-Berghaus J et al (2006) Method and apparatus for fine particle liquid suspension feed for thermal spray system and coatings formed therefrom, Patent US 20060289405 A1 and method and system for producing coatings from liquid feedstock using axial feed, Patent US 20110237421 A1, Licenced to Northwest Mettech Corp
69. Salpeter EE (1961) Electron density fluctuations in a plasma. Phys Rev 122:1663
70. Dzierżega K, Mendys A, Pokrzywk B (2014) What can we learn about laser-induced plasmas from Thomson scattering experiments. Spectrochim Acta Part B 98:76–86
71. Schein J, Hartz-Behrend K, Kirner S, Kühn-Kauffeldt M, Bachmann B, Siewert E (2015) New methods to look at an old technology: innovations to diagnose thermal plasmas. Plasma Chem Plasma Process 35:437–453
72. Fauchais P, Coudert JF, Vardelle M (1989) Diagnostics in thermal plasma processing. In Auciello O, Flamm DL (eds) Plasma diagnostics, vol 1. Academic, pp 349–446
73. Fauchais P et al (1992) Diagnostics of thermal spraying plasma jets. J Therm Spray Technol 1(2):117–128
74. Chen WLT, Heberlein J, Pfender E (1994) Diagnostics of a thermal plasma jet by optical emission spectroscopy and enthalpy probe measurements. Plasma Chem Plasma Process 14(3):317–322
75. Baronnet JM (1971) Comparative study of measurement methods to determine rotational and vibrational temperatures of N_2 molecule in nitrogen plasma produced by a DC arc, Univ. of Poitiers April 30 (in French)
76. Vardelle M, Trassy C, Vardelle A, Fauchais P (1991) Experimental investigation of powder vaporization in thermal plasma jets. Plasma Chem Plasma Process 11(2):185–201

77. Eckbreth AC, Anderson TJ (1985) Dual broadband CARS for simultaneous multiple species measurements. Appl Opt 24:2731–2736
78. Grey J, Jacobs PF, Sherman MP (1962) Calorimetric probe for the measurement of extremely high temperatures. Rev Sci Instrum 33(7):738–741
79. Brossa M, Pfender E (1988) Probe measurements in thermal plasma jets. Plasma Chem Plasma Process 8(1):75–90
80. Capetti A, Pfender E (1989) Probe measurements in argon plasma jets operated in ambient argon. Plasma Chem Plasma Process 9(2):329–341
81. Mauer G, Vaßen R, Stöver D (2011) Plasma and particle temperature measurements in thermal spray: approaches and applications. J Therm Spray Technol 20(3):391–406
82. Coudert JF, Planche MP, Fauchais P (1995) Velocity measurement of DC plasma based on arc root fluctuations. Plasma Chem Plasma Process 15(1):47–70
83. Planche MP, Coudert JF, Fauchais P (1998) Velocity measurements for arc jets produced by a DC plasma spray torch. Plasma Chem Plasma Process 18(2):263–283
84. Landes K (2006) Diagnostics in plasma spraying techniques. Surf Coat Technol 201:1948–1954
85. Schein J, Richter M, Landes KD, Forster G, Zierhut J, Dzulko M (2008) Tomographic investigation of plasma jets produced by multielectrode plasma torches. J Therm Spray Technol 17(3):338–343
86. Malmberg S, Heberlein J (1993) Effect of plasma spray operating conditions on plasma jet characteristics and coating properties. J Therm Spray Technol 2(4):339–344
87. Fauchais P, Vardelle A (2000) Heat, mass and momentum transfer in coating formation by plasma spraying. Int J Therm Sci 39:852–870
88. Pfender E, Chen WLT, Spores R (1990) A new look at the thermal and gas dynamic characteristics of a plasma jet. In: Berndt CC (ed) Proc. proceedings of the 3rd national thermal spray conference. ASM International, Long Beach, pp 1–10
89. Fincke JR, Haggard DC, Swank WD (2001) Particle temperature measurement in the thermal spray process. J Therm Spray Technol 10(2):255–266
90. Wang P, Yu SCM, Ng HW (2007) Correlation of plasma sprayed coating deposition efficiency with volume flux measurements by phase doppler anemometry (PDA). Plasma Chem Plasma Process 27:311–336
91. Moreau C, Gougeon P, Lamontagne M, Lacasse V, VaudreuilG , Cielo P (1994) On-line control of the plasma spraying process by monitoring the temperature, velocity and trajectory of in-flight particles. In: Berndt CC, Sampath S (ed) Thermal spray industrial applications. ASM International, Materials Park, pp 431–437
92. Fauchais P, Vardelle M (2010) Sensors in spray processes. J Therm Spray Technol 19(4):668–694
93. Renouard-Vallet G (2004) Elaboration by plasma spraying of dense and thin (a few tens of micro meters) yttria stabilized zirconia electrolytes for SOFCs. PhD thesis, University of Limoges France, Feb. 8 (in French)
94. Mauer G, Vaßen R, Stöver D (2007) Comparison and applications of DPV-2000 and accuraspray-g3 diagnostic systems. J Therm Spray Technol 16(3):414–424
95. Fauchais P (2004) Understanding plasma spraying. J Phys D Appl Phys 37:86–108
96. Vardelle A, Vardelle M, Fauchais P (1982) Influence of velocity and surface temperature of alumina particles on the properties of plasma sprayed coatings. Plasma Chem Plasma Process 2(3):255–291
97. Vardelle M, Vardelle A, Fauchais P, Li K-I, Dussoubs B, Themelis NJ (2001) Controlling particle injection in plasma spraying. J Therm Spray Technol 10(2):267–284
98. Pfender E (1988) Fundamental studies associated with the plasma spray process. Surf Coat Technol 34:1–14
99. McKelliget J, Szekely J, Vardelle M, Fauchais P (1982) Temperature and velocity fields in a gas stream exiting a plasma torch, a mathematical model and its experimental verification. Plasma Chem Plasma Process 2(3):317–332
100. Legros E (2003) Contribution to 3D modeling of the plasma spray process and application to a two torches to produce a liquid film of alumina (in French), PhD thesis Nb. 55-2003, Univ. of Limoges
101. Pfender E, Fincke J, Spores R (1991) Entrainment of cold gas into thermal plasma jets. Plasma Chem Plasma Process 11(4):529–543
102. Pfender E (1994) Plasma jet behavior and modeling associated with the plasma spray process. Thin Solid Films 238:228–241
103. Roumilhac P, Coudert J-F, Fauchais P (1990) Influence of the arc chamber design and the surrounding atmosphere on the characteristics and temperature distribution of Ar–H_2 and Ar–He spraying plasma jets. In: Apelian D, Szekely J (eds) Plasma processing and synthesis of materials, vol 190. MRS, Pittsburgh, pp 227–333

104. Huang PC, Heberlein J, Pfender E (1995) A two-fluid model of turbulence for a thermal plasma jet. Plasma Chem Plasma Process 15(1):25–46
105. Trelles JP, Pfender E, Heberlein JVR (2006) Multiscale finite element modeling of arc dynamics in a DC plasma torch. Plasma Chem Plasma Process 26:557–575
106. Moreau E, Chazelas C, Mariaux G, Vardelle A (2006) Modeling the restrike mode operation of a DC plasma spray torch. J Therm Spray Technol 15(4):524–530
107. Trelles JP, Pfender E, Heberlein JVR (2007) Modeling of the arc reattachment process in plasma torches. J Phys D Appl Phys 40(2007):5635–5648
108. Huang R, Fukanuma H, Uesugi Y, Tanaka Y (2012) Simulation of arc root fluctuation in a DC non-transferred plasma torch with three dimensional modeling. J Therm Spray Technol 21(3–4):636–643
109. He-Ping Li, Pfender E (2007) Three dimensional modeling of the plasma spray process. J Therm Spray Technol 16(2):245–260
110. Trelles JP, Chazelas C, Vardelle A, Heberlein JVR (2009) Arc plasma torch modeling. J Therm Spray Technol 18(5–6):728–752
111. Selvan B, Ramachandran K (2009) Comparisons between two different three-dimensional arc plasma torch simulations. J Therm Spray Technol 18(5–6):846–857
112. Alaya M, Chazelas C, Vardelle A (2016) Parametric study of plasma torch operation using a MHD model coupling the arc and electrodes. J Therm Spray Technol 25(1–2):36–43
113. Chyou YP, Pfender E (1989) Modeling of plasma jets with superimposed vortex flow. Plasma Chem Plasma Process 9(2):291–328
114. Lapierre D, Kearney RJ, Vardelle M, Vardelle A, Fauchais P (1994) Effect of a substrate on the temperature distribution in an argon–hydrogen thermal plasma jet. Plasma Chem Plasma Process 14(4):407–423
115. Kang CW, Ng HW, Yu SCM (2006) Comparative study of plasma spray flow fields and particle behavior near to flat inclined substrates. Plasma Chem Plasma Process 26:149–175
116. Ba T, Kang CW, Ng HW (2009) Numerical study of the plasma flow field and particle in-flight behavior with the obstruction of a curved substrate. J Therm Spray Technol 18(5–6):858–874
117. Rahmane M, Soucy G, Boulos MI, Henne R (1998) Fluid dynamic study of direct current plasma jets for plasma spraying applications. J Therm Spray Technol 7(3):349–356
118. Jankovic M, Mostaghimi J, Pershin V (2000) Design of a new nozzle for direct current plasma guns with improved spraying parameters. J Therm Spray Technol 9(1):114–120
119. Gleizes A (2015) Perspectives on thermal plasma modeling. Plasma Chem Plasma Process 35:455–469
120. Bobzin K, Öte M (2016) Modeling multi-arc spraying systems. J Therm Spray Technol 25(5):920–932
121. Xi Chen, Pfender E (1982) Heat transfer to a single particle exposed to a thermal plasma. Plasma Chem Plasma Process 2(2):185–212
122. Pfender E, Lee YC (1985) Particle dynamics and particle heat and mass transfer in thermal plasmas. Part I. The motion of a single particle without thermal effects. Plasma Chem Plasma Process 5(3):211–237
123. Lee YC, Chyou YP, Pfender E (1985) Particle dynamics and particle heat and mass transfer in thermal plasmas. Part II. Particle heat and mass transfer in thermal plasmas. Plasma Chem Plasma Process 5(4):391–414
124. Chen X, Chyou YP, Lee YC, Pfender E (1985) Heat transfer to a particle under plasma conditions with vapor contamination from the particle. Plasma Chem Plasma Process 5(2):119–141
125. Pfender E (1989) Particle behavior in thermal plasmas I. Plasma Chem Plasma Process 9(1):167S–194S
126. Chyou YP, Pfender E (1989) Behavior of particulates in thermal plasma flows. Plasma Chem Plasma Process 9(1):45–71
127. Boulos MI, Fauchais P, Vardelle A, Pfender E (1993) Fundamentals of plasma particle momentum and heat transfer. In: Suryanarayanan R (ed) Plasma spraying theory and applications. World Scientific, Singapore
128. Lee YC, Chyou YP, Pfender E (1997) Particle dynamics and particle heat and mass transfer in thermal plasmas. Part III. Thermal plasma jet reactors and multi-particle injection. Plasma Chem Plasma Process 7(1):1–27
129. Pfender E, Chang CH (1998) Plasma spray jets and plasmaparticulate interaction: modeling and experiments. In Coddet C (ed) Thermal spray: meeting the challenges of the 21st century, vol 1. ASM Int. Materials Park, pp 315–321
130. Clift R, Grace JR, Weber JE (1978) Bubbles, drops and particles. Academic Press, New York
131. White FM (1974) Viscous fluid flow. McGraw Hill, New York
132. Rudinger G (1980) Fundamentals of gas-solid particle flow. Elsevier, Amsterdam

133. Vardelle M, Vardelle A, Fauchais P, Boulos MI (1983) Plasma-particle momentum and heat transfer: modeling and measurements. AIChE J 9(2):236–243
134. Lewis JW, Gauvin WH (1973) Motion of particles entrained in a plasma jet. AIChE J 19(6):982–990
135. Chen X, Pfender E (1983) Behavior of small particles in a thermal plasma flow. Plasma Chem Plasma Process 3(3):351–366
136. Vardelle A, Themelis NJ, Dussoubs B, Vardelle M, Fauchais P (1997) Transport phenomena in thermal plasmas. J High Temp Mater Process 1(3):295–317
137. Ganser GH (1993) A rational approach to drag prediction of spherical and nonspherical particles. Powder Technol 77:143–152
138. Bisson JF, Moreau C (2003) Effect of plasma fluctuations on inflight particle parameters. J Therm Spray Technol 12(2):38–43
139. Vardelle A (1988) Numerical study of heat, momentum and mass transfers between an arc plasma at atmospheric pressure and solid particles, Thesis of doctorate, Univ. of Limoges, July (1988)
140. Fizdon JK (1979) Melting of powder grains in a plasma flame Int. J Heat Mass Transf 22:749–761
141. Sayegh NN, Gauvin WH (1979) Analysis of variable property heat transfer to a single sphere in high temperature surrounding. AIChE J 25:522–534
142. Bourdin E, Fauchais P, Boulos MI (1983) Transient heat conduction under plasma conditions. Int J Heat Mass Transf 26:567–582
143. Fizdon JK (1979) Melting of powder grains in a plasma flame. Int J Heat Mass Transf 22:749–761
144. Dallaire S (1982) Influence of temperature on the bonding mechanism of plasmasprayed coatings. Thin Solid Films 95:237–241
145. Lee YC, Hsu C, Pfender E (1981) Modelling of particle injection into a DC plasma jet. In: 5th international symposium on plasma chemistry, vol 2, Edinburgh, pp 795–801
146. Chen XI, Pfender E (1982) Unsteady heating and radiation effects of small particles in a thermal plasma. Plasma Chem Plasma Process 2:293–316
147. Fauchais P, Montavon G, Bertrand G (2010) From powders to thermally sprayed coatings. J Therm Spray Technol 19(1–2):56–80
148. Hurevich V, Smurnov I, Pawlowski L (2002) Theoretical study of the powder behavior of porous particles in a flame during plasma spraying. Surf Coat Technol 151–152:370–376
149. Chen X, Pfender E (1983) Effect of the Knudsen number on heat transfer to a particle immersed into a thermal plasma. Plasma Chem Plasma Process 3:113–397
150. Essoltani A, Proulx P, Boulos MI, Gleizes A (1994) Effect of the presence of iron vapors on the volumetric emission of Ar/Fe and Ar/Fe/H2 plasmas. Plasma Chem Plasma Process 14(3):301–315
151. Neiser RA, Smith MF, Dykhuisen RC (1998) Oxidation in wire HVOF-sprayed steel. J Therm Spray Technol 7(4):537–545
152. Espié G, Fauchais P, Hannoyer B, Labbe JC, Vardelle A (1999) Effect of metal particles oxidation during the APS on the wettability. In: Fauchais P, Van der Mullen J, Heberlein J (eds) Heat and mass transfer under plasma condition, in Annals of NY Academy of Sciences, vol 891, pp. 143–151
153. Seyed AA, Denoirjean A, Denoirjean P, Labbe JC, Fauchais P (2005) In-flight oxidation of stainless steel in plasma spraying. J Thermal Spray Technol 14(1):124–177
154. Proulx P, Mostaghimi J, Boulos MI (1987) Heating of powders in an RF inductively coupled plasma under dense loading conditions. Plasma Chem Plasma Process 7(1):29–52
155. Vincenzi L, Suzuki S, Outcalt D, Heberlein J (2010) Controlling spray torch fluid dynamics—effect on spray particle and coating characteristics. J Therm Spray Technol 19(4):713–722
156. Fauchais P, Fukumoto M, Vardelle A, Vardelle M (2004) Knowledge concerning splat formation: an invited review. J Therm Spray Technol 13(3):337–360
157. Chandra S, Fauchais P (2009) Formation of solid splats during thermal spray deposition. J Therm Spray Technol 18(2):148–180
158. Shinoda K et al (2007) High-speed thermal imaging of yttria-stabilized zirconia droplet impinging on substrate in plasma spraying. Appl Phys Lett 90:194103
159. McDonald A, Lamontagne M, Chandra S, Moreau C (2006) Photographing impact of plasma sprayed particles on metal substrates. J Therm Spray Technol 15(4):708–716
160. Gifford DJ, Pollard L, Wuest G, Fletcher RC (2003) Thermal spray booth design guidelines. In: Prepared by the ASM-TSS safety committee. ASM Int. Materials Park, p 47
161. Goutier S, Vardelle M, Labbe JC, Fauchais P (2011) Flattening and cooling of millimeter- and micrometer-sized alumina drops. J Therm Spray Technol 20(1–2):59–67
162. Goutier S, Vardelle M, Fauchais P (2013) Comparison between metallic and ceramic splats: influence of viscosity and kinetic energy on the particle flattening. Surf Coat Technol 235:657–668
163. Fauchais P, Vardelle M, Goutier S (2016) Latest researches advances of plasma spraying: from splat to coating formation. J Therm Spray Technol 25(6):1087–1107

164. Bahbou MF, Nylén P (2007) On-line measurement of plasma-sprayed Ni-particles during impact on a Ti-surface: influence of surface oxidation. J Therm Spray Technol 16(4):506–511
165. Mehdizadeh NZ, Chandra S, Mostaghimi J (2002) Effect of substrate temperature and roughness on coating formation. In: Lugscheider E (ed) Proc. ITSC 2002. DVS, Düsseldorf, pp 830–837